

Article

Influence of RDF Composition on Mercury Release during Thermal Pretreatment

Marcelina Bury ^{1,*} , Tadeusz Dziok ¹ , Karel Borovec ²  and Piotr Burmistrz ¹ 

¹ Faculty of Energy and Fuels, AGH University of Science and Technology, Al. A. Mickiewicza 30, 30-059 Krakow, Poland

² Energy Research Center VŠB, Technical University of Ostrava, 17. Listopadu 15/2172, 708-33 Ostrava, Czech Republic

* Correspondence: bury@agh.edu.pl; Tel.: +48-(12)-617-29-06

Abstract: The growing world population is contributing to the increasing amounts of waste and a significant increase in energy demand. Therefore, coal will increasingly be replaced by refuse-derived fuel (RDF), which is produced from municipal solid waste. The use of such fuel poses many difficulties because of its heterogeneity and high mercury emission. One method to stabilize the properties of RDF and reduce the mercury content is thermal pretreatment. The purpose of this study was to investigate the release of mercury from RDF samples following thermal pretreatment. The study was carried out in the temperature range of 100–350 °C. Statistical analysis was performed on the correlation between the composition of the RDF samples and the release of mercury. The RDF samples showed a very high variation in the mercury content, ranging from 45 to 849 µg Hg/kg (1.7 to 35.3 µg Hg/MJ). Thermal pretreatment removed a significant amount of mercury at 250 °C (94–99%). Paper content positively affected mercury release. Relatively low correlation coefficients were obtained in the statistical analysis, which may be explained by the significant heterogeneity of the RDF samples magnified by the variability in the mercury content within particular fractions.

Keywords: mercury; mercury removal; thermal pretreatment; alternative fuels; waste; RDF



Citation: Bury, M.; Dziok, T.; Borovec, K.; Burmistrz, P. Influence of RDF Composition on Mercury Release during Thermal Pretreatment. *Energies* **2023**, *16*, 772. <https://doi.org/10.3390/en16020772>

Academic Editor: Jamie W.G. Turner

Received: 1 December 2022

Revised: 30 December 2022

Accepted: 4 January 2023

Published: 9 January 2023



Copyright: © 2023 by the authors. Licensee MDPI, Basel, Switzerland. This article is an open access article distributed under the terms and conditions of the Creative Commons Attribution (CC BY) license (<https://creativecommons.org/licenses/by/4.0/>).

1. Introduction

The growing world population is contributing to increasing amounts of municipal and industrial waste being generated. It is predicted that by 2050, 3.4 billion tonnes of waste will be generated globally per year, which is an increase of 70% over the current level (2.0 billion tonnes) [1]. At the same time, the energy demand will increase significantly [2]. Fossil fuels will increasingly be replaced by alternative fuels, such as refuse-derived fuel (RDF) and solid-recovered fuel (SRF) [3]. They are produced from the combustible fraction of municipal solid waste (MSW). The fraction of municipal solid waste that can be used to produce RDF is mixed municipal solid waste (waste generated by the municipal and household sectors). The fraction of mixed municipal solid waste is segregated, shredded, and dried [4]. In Poland, the RDF production process is carried out by the RIPOK (Polish Regional Municipal Waste Processing Plants). The final stage of RDF production is forming it into briquettes or pellets [4]. This type of fuel is composed of six main morphological fractions: paper, cardboard, plastics, textiles, aluminum, and others (which cannot be classified) [5]. SRF is produced from non-hazardous waste and is standardized by the European Committee for Standardization (CEN). The classification parameters are calorific values as well as mercury and chlorine content [6].

Compared with raw municipal solid waste, RDF is characterized by more homogeneity, higher calorific value (19–31 MJ/kg dry basis), lower ash content (8–20% dry basis) [7], and optimum moisture content (20%) to undergo pelletization [8]. In addition, RDF is expected to have a particle size suitable for consumers. For example, for co-combustion with coal in

a pulverized boiler, RDF fuel should have a particle size of less than 200 μm , with 60–70% of the fuel in the range of 90–200 μm [9].

The main consumer of RDF in the world is the cement industry [10]. In Poland, the main consumers of RDF are also cement plants [11], which use about 1.2–1.5 million Mg of waste per year, as well as combined heat and power plants co-firing coal and waste [12]. RDF combustion instead of coal can reduce emissions. This can be achieved through the use of appropriate flue gas cleaning systems, which are enforced by relevant regulations [13,14]. Technologies for its thermochemical conversion, such as pyrolysis [15] and gasification [16], are also being developed.

The use of alternative waste-derived solid fuels poses many difficulties because of their heterogeneity, unstable physicochemical properties, technological and operational problems, and the environmental hazards resulting from increased emissions [17], including mercury [7]. The mercury released through the RDF combustion process is emitted into the atmosphere. There is a biochemical cycle of mercury in the ecosystem. Through dry and wet deposition processes, mercury passes into water and soil, where it is methylated. Toxic methylmercury is highly bioaccumulated by plants and animals. Thus, the emitted mercury enters the human food chain. This poses a real threat to human life and health [18]. The mercury content in waste varies widely, and co-combusting it with coal may cause emission standards to be exceeded [7]. Such standards were introduced in 2021 in the European Union for large combustion plants [19]. Furthermore, consumers of RDF have their own specific quality requirements regarding the calorific value, moisture content, [20] or mercury content [21].

One method for improving and stabilizing the properties of RDF is the thermal pretreatment process (low-temperature pyrolysis) [22]. This process is used to enhance the properties of other types of waste as well [23,24]. In the case of RDF thermal pretreatment can provide higher calorific value [25], lower chlorine content, and significantly lower mercury content [26]. However, no detailed studies of the influence of RDF composition (including morphology) on the release of mercury during the pyrolysis process have been conducted. The thermal pretreatment process has many advantages over other available methods for releasing mercury from RDF. One of the methods is blending with another type of fuel that is characterized by a relatively low mercury content [7]. Biomass or high-quality waste-derived fuel (SRF type) can be used for this purpose [27]. However, a limitation of this method is the final mercury content of the blend. In the case of RDF characterized by a very high mercury content of 79.3 $\mu\text{g}/\text{MJ}$ [7], blending even with torrefied biomass (mercury content of 0.6 $\mu\text{g}/\text{MJ}$ [28]) may not be effective. Moreover, the use of high-quality solid fuels will generate additional costs. Another method is the RDF segregation process to separate a fraction that meets the requirements for SRF. The disadvantage of this method is the reduction in the mass of fuel (reduction in chemical enthalpy) and the generation of an additional waste stream with a higher mercury content, which has to be utilized. The process of mercury removal from waste in the thermal pretreatment process has not been studied enough, as it has been for coal and biomass. An important issue is the different origins of the particular types of waste and their heterogeneity. The sources of mercury in waste are also varied, i.e., dyes [29], biocides [30], ink [31], and catalysts in the production process [32]. It was noted that the type of waste determines the process of mercury release [33]. However, no studies have been conducted on the effect of the content of the various waste fractions on the release of mercury from RDF. The purpose of this study was to investigate the release of mercury from the RDF samples derived from municipal solid waste with different morphological compositions, characteristics (the content of sulfur, ash, and volatile matter), and mercury content. The effect of mass loss was also analyzed. The study was carried out in the temperature range of 100–350 $^{\circ}\text{C}$ until mercury was almost completely released [33]. To determine the influence of the mentioned parameters on the process of mercury release from RDF, a statistical analysis was carried out.

2. Materials and Methods

2.1. Examined Samples

Six samples of RDF produced from municipal solid waste in Polish companies were taken for examination. The mass of the bulk sample was approximately 6 kg. Prior to the examination, the fuel samples were dried at room temperature.

2.2. Determination of the Morphological Composition of the RDF Samples

The examined RDF samples were separated into six fractions: plastic foil, plastics, waste paper, textiles, aluminum, and others (which could not be classified). The particular fractions were weighed and compared with the initial mass of the sample. The morphological composition of the samples is shown in Table 1. An RDF sample with a relatively large particle size (less than 50 mm) was selected for examination. This enabled the manual separation of individual waste fractions: plastic foils, plastics, waste paper, textiles, and aluminum. Fine fractions that could not be classified were assigned to the group labeled other.

Table 1. Morphological composition of RDF samples.

Sample Number	Share of Fractions Separated (%)					
	Plastic Foil	Plastics	Waste Paper	Textiles	Aluminum	Other
RDF-1	50.0	22.8	2.9	2.0	1.0	21.3
RDF-2	21.5	30.2	15.6	29.0	2.7	1.0
RDF-3	25.6	23.9	25.2	22.7	0.0	2.6
RDF-4	35.2	16.8	20.9	18.4	4.0	4.7
RDF-5	16.4	40.1	18.3	21.4	3.7	0.1
RDF-6	18.2	38.8	3.5	1.5	1.8	36.3
Average	27.7	28.8	14.4	15.8	2.2	11.1

2.3. Sample Preparation

The RDF samples were remixed, homogenized, and ground for laboratory examination, using a Freezer/Mill 6870D cryogenic mill from SpexSamplePrep. The standards for waste analysis require a particle size below 1.0 mm. To increase the homogeneity of the laboratory sample and the precision of the obtained results, the RDF samples were milled to a particle size below 0.5 mm.

2.4. Characterization of the RDF Samples

The proximate and ultimate analyses of the RDF samples were performed, including the determination of the mercury content. The methodology of this analysis is shown in Table 2, and the characteristics of the samples are shown in Table 3. Table 3 also presents the mercury content related to the lower calorific values ($Hg_{ad}/q_{p,net,ad}$).

Table 2. Methods of examining the samples.

Parameter	Method of Measurement	Principle behind the Method	Procedure/Standard
Moisture (M_{ad})	Moisture balance MA 110.R by Radwag	Gravimetric method	Standard PN-ISO 589:2006
Ash (A_{ad})	Muffle furnace: 550 °C	Gravimetric method	PN-EN 15403:2011
Volatile matter (V_{ad})	Muffle furnace: 900 °C	Gravimetric method	PN-EN 15402:2011

Table 2. Cont.

Parameter	Method of Measurement	Principle behind the Method	Procedure/Standard
Gross calorific value ($q_{v,gr,ad}$)	IKA C 6000 calorimeter by ELTRA	Combustion in a calorimetric bomb in oxygen at a pressure of 3 MPa	ISO 1928
Carbon (C_{ad})	CHS-580 analyzer by ELTRA	High-temperature combustion method	PKN-ISO/TS 12902:2007
Hydrogen (H_{ad})	CHS-580 analyzer by ELTRA	High-temperature combustion method	PKN-ISO/TS 12902:2007
Sulfur ($S_{t,ad}$)	CHS-580 analyzer by ELTRA	High-temperature combustion method	Standard ASTM D-4239
Mercury (Hg_{ad})	DMA-80 mercury analyzer by Milestone	Atomic absorption spectrometry	Milestone procedure

Table 3. Characteristics of the samples.

Sample Number	Proximate Analysis				Ultimate Analysis				
	M_{ad} (%)	A_{ad} (%)	V_{ad} (%)	$q_{p,net,ad}$ (MJ/kg)	C_{ad} (%)	H_{ad} (%)	$S_{t,ad}$ (%)	Hg_{ad} (μ g/kg)	$Hg_{ad}/q_{p,net,ad}$ (μ g/MJ)
RDF-1	1.1	11.0	87.66	33.538	71.4	13.40	0.07	56	1.7
RDF-2	2.9	17.2	70.46	23.713	56.0	8.44	0.64	764	32.2
RDF-3	2.5	12.0	78.41	24.077	52.8	7.19	0.16	849	35.3
RDF-4	3.1	19.6	75.14	18.022	47.6	6.22	0.32	89	4.9
RDF-5	1.9	11.7	78.50	26.916	59.2	8.41	0.11	686	25.5
RDF-6	3.3	21.8	62.84	16.623	40.5	6.39	0.25	45	2.7

2.5. Procedure for Thermal Pretreatment of RDF Samples

Mercury is characterized by very high volatility, and the process is intensified in higher temperatures. This is the main parameter determining the release of mercury from waste [33]. To maximize mercury removal, a purge gas was used to wash out the mercury released from the sample. This reduced the phenomenon of mercury resorption on sample particles. The process of mercury release is determined by the forms of mercury occurrence in waste. These may be organic and mineral compounds or elemental mercury [34]. Depending on the form, mercury can be released via thermal decomposition, sublimation, or evaporation [35].

To provide the complete mercury release from the analyzed RDF samples based on previous experience [33,36], the equipment and process parameters were properly selected. The thermal pretreatment process was performed with the laboratory equipment shown in Figure 1. The RDF sample was placed in a quartz boat and introduced into a horizontal tube furnace to a set temperature (100 or 150 or 200 or 250 or 300 or 350 °C). The mass of the sample was 0.2 to 0.3 g, depending on its bulk density. The temperature of the sample was controlled continuously. After the sample had reached the set temperature (which took place after about 4 min), it was kept at this temperature for another 30 min. After being cooled, the samples were weighed, and the mercury content was determined. Thermal pretreatment was carried out in an argon stream with a flow rate of 500 cm³/min. The mercury removal method was developed on the basis of previous work [33].

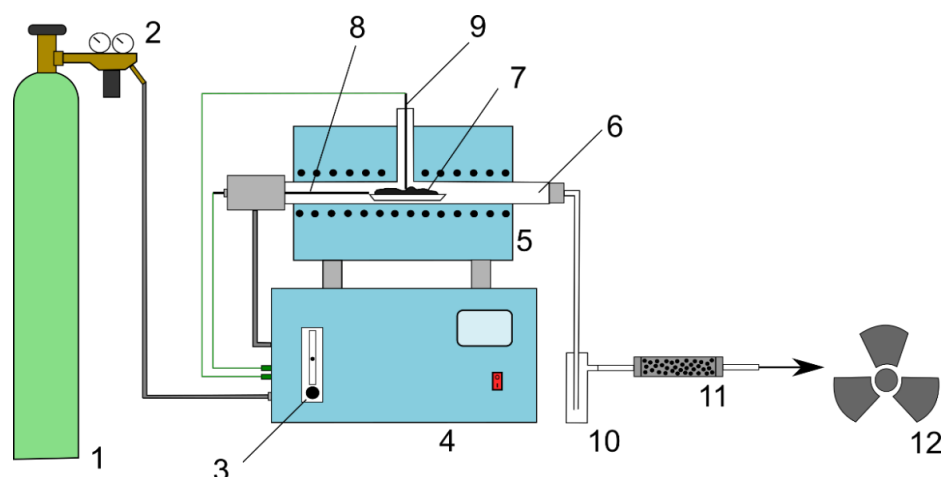


Figure 1. Equipment for the thermal pretreatment of waste: 1—argon cylinder; 2—gas reducer; 3—control valve; 4—furnace heating control system; 5—tube furnace; 6—quartz reactor; 7—boat with sample; 8—thermocouple controlling the temperature of the furnace; 9—thermocouple controlling the temperature of the sample; 10—cooler; 11—activated carbon filter; 12—laboratory exhaust.

To estimate the amount of mercury released, the ΔHg (%) index, calculated according to Equation (1), was used.

$$\Delta Hg = \frac{Hg_0 - Hg_t \cdot \frac{100 - \Delta m}{100}}{Hg_0} \times 100, \quad (1)$$

where

ΔHg is the mercury release index (%);

Δm is the mass loss of the sample (%);

Hg_0 is the mercury content in the raw sample ($\mu\text{g}/\text{kg}$);

Hg_t is the mercury content in the sample after thermal treatment ($\mu\text{g}/\text{kg}$).

2.6. Procedure for Statistical Analysis

Statistical analysis of the correlation between the composition of the examined RDF samples (morphological composition according to Table 1 and the content of ash, volatile matter, sulfur, and mercury according to Table 3) and the amount of mercury released, as well as the activation energy of the mercury release was carried out in two stages. An analysis of Spearman's rank correlation coefficients (Stage I) and linear correlation coefficients (Stage II) was performed. In Stage I, Spearman's rank correlation coefficients were determined for all relationships and were verified using the critical value of the test at the significance level of $\alpha = 0.05$. In Stage II, the linear correlation coefficients were determined for the cases for which Spearman's rank correlation coefficient was significant. The significance of the correlation coefficients was verified using the F-Snedecor test for a significance level of $\alpha = 0.05$. Additionally, the test probability (p -value) was determined.

3. Results and Discussion

3.1. Analysis of the Mercury Content in the RDF Samples

The mercury content in the RDF samples ranged from 45 to 849 $\mu\text{g Hg}/\text{kg}$ (with an average of 487 $\mu\text{g Hg}/\text{kg}$). The mercury content related to the lower calorific value ranged from 1.7 to 35.3 $\mu\text{g Hg}/\text{MJ}$ and was typical of alternative solid fuels produced from waste [7]. Regarding the mercury content, the examined RDF samples can be divided into two groups: those with a low mercury content, from 1.7 to 4.9 $\mu\text{g Hg}/\text{MJ}$ (Samples RDF-1, RDF-4, and RDF-6), and those with a high mercury content, from 25.5 to 35.3 $\mu\text{g Hg}/\text{MJ}$ (Samples RDF-2, RDF-3, and RDF-5). The mercury content in the RDF samples from the first group was similar to that of high-quality sub-bituminous coal derived from the washing

processes. In contrast, the mercury content in the RDF samples from the second group was similar to that of lignite [7,37]. According to the classification of SRF, the samples from the first group could be classified as Class 1 and those from the second group as Class 2 or 3 in terms of their mercury content [27].

The morphological composition of RDF determines the mercury content. For example, textiles have a mercury content of 8–375 $\mu\text{g Hg/kg}$ [7,38], paper has 9–78 $\mu\text{g Hg/kg}$ [36], and plastics have 1–1648 $\mu\text{g Hg/kg}$ [39]. Nevertheless, no clear influence of morphological composition on mercury content was observed. This may be explained by the significant variability in the mercury content in different types of waste. However, it was noted that RDF samples with low mercury content were characterized by a relatively high content of fine fraction (from 4.7% to 36.3%—other fraction according to Table 1).

It can be postulated that appropriate waste management can be very useful in reducing mercury emissions from coal combustion processes in coal-fired power plants. This can be achieved by substituting low-quality lignite and sub-bituminous coals with low-mercury RDF. For RDF with high mercury content, additional methods will be required to remove mercury from the flue gases [40,41]. There is also a potential for mercury release from RDF before combustion. This can be achieved through a low-temperature pyrolysis process.

3.2. Effect of Temperature on the Release of Mercury from the RDF Samples

Figure 2 shows the mercury release from the RDF samples in the temperature range of 100–350 °C. Despite the differences in the characteristics of the samples, in all cases, mercury started to be released at 100 °C, and by 250 °C, there was an almost complete release (94–99%). Further increases in temperature did not result in a significant increase in mercury release. Significant differences in mercury release were observed in the temperature range of 100–250 °C. As previously mentioned, there was no clear effect of the morphological composition (Table 1) or characteristics of the samples (Table 3). To investigate the effect of the composition of the RDF samples on mercury release in detail, statistical analysis was performed. The results are presented in Section 3.4.

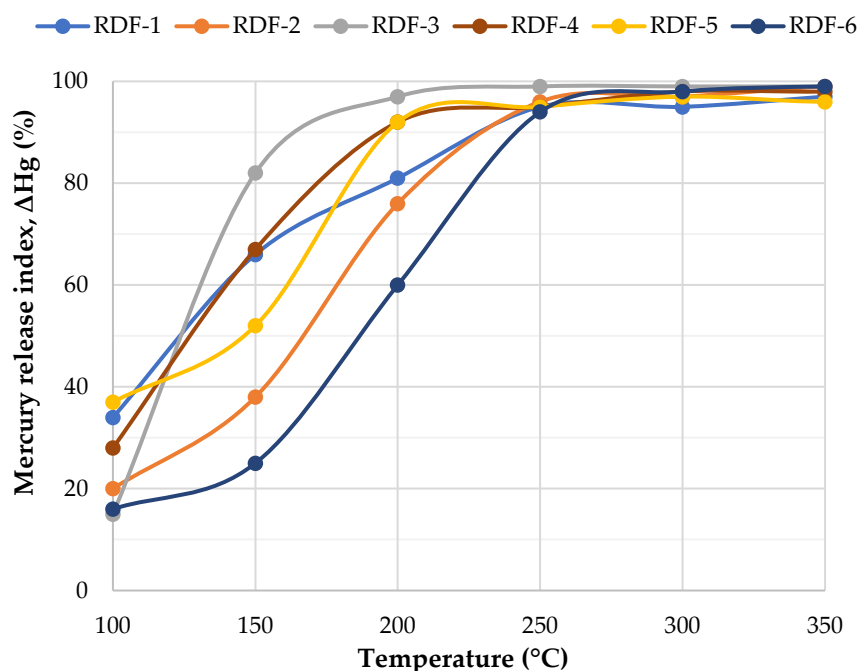


Figure 2. Release of mercury from the RDF samples during thermal pretreatment (purge gas flow: 500 cm^3/min ; residence time: 30 min).

The largest difference was observed between Samples RDF-3 and RDF-6, which demonstrated the fastest and the slowest release of mercury, respectively (Figure 2). In addition, Sample RDF-3 had the highest mercury content (849 $\mu\text{g Hg/kg}$), while Sample RDF-6 had the lowest (45 $\mu\text{g Hg/kg}$). This suggests that RDF can contain large amounts of mercury, which is characterized by a low release temperature (for Sample RDF-3, 82% of the mercury was released at 150 $^{\circ}\text{C}$). It was also observed that with a similar content of plastics (plastic foil and plastics) in both samples, Sample RDF-3 was characterized by a significantly higher content of textiles and waste paper. In accordance with our previous work [33,36], mercury was very easily released from various types of paper and from textiles. Table 4 shows literature data on mercury release from solid waste in the thermal pretreatment process.

Table 4. Literature data on mercury release from solid waste in the thermal pretreatment process.

Waste Type	Mercury Release (%)	Temperature of Thermal Pretreatment ($^{\circ}\text{C}$)	Ref.
RDF	96	250	[33]
RDF + demolition and construction wood	82	220	[26]
Sewage sludge + MSW	80	300	[42]
Sewage sludge	91	250	[33]
Paper	63–93	300	[33,36]
Cardboards	93	300	[33]
Plastics	48	350	[33]
Plastic foils	81	300	[33]
Textiles	94	250	[33]
Car tires	85	300	[33]
Mercury-containing waste from various industrial facilities	97	400	[43]

It should be emphasized that both the morphological composition and mercury content in RDF determine the behavior of mercury in thermal treatment processes. Mercury may occur in different morphological fractions in different forms, depending on the technological process by which it is produced. For example, in textiles, mercury is found in dyes and biocides [30,44]. In plastics, mercury is used in red pigment or can be used as a catalyst in the production process [32]. In paper, mercury is found mainly in ink [31]. The lack of a significant influence of the morphological composition of RDF on the release of mercury may suggest similar thermal characteristics of mercury compounds found in the different morphological fractions.

The thermal pretreatment allowed the mercury content to be significantly lower: less than 37 $\mu\text{g Hg/kg}$. In the case of the RDF samples in the second group (RDF-2, RDF-3, and RDF-5), the process changed the mercury content classification from SRF Class 2 and 3 to Class 1 (below 1.6 $\mu\text{g Hg/MJ}$).

The characteristics of individual RDF samples determined the thermal pretreatment process. Differences in the decomposition of organic matter were observed, resulting in different mass losses. The mass loss of the sample increased with the increasing process temperature. At 250 $^{\circ}\text{C}$, it ranged from 3% (RDF-1) to 13% (RDF-6). It was related to the content of plastics (plastics and plastic foil). Furthermore, for samples characterized by a high plastic content at higher temperatures, the melting of the sample was observed. The content of volatile matter and ash did not determine mass loss. Mass loss is an advantage of low-temperature pyrolysis processes over high-temperature processes. At higher temperatures, the mass loss is much higher, as high as 41% (in the temperature range of 350–600 $^{\circ}\text{C}$) or even 59% (in a temperature range of 750–850 $^{\circ}\text{C}$) [45]. This results in a significant loss of the chemical enthalpy of the fuel.

3.3. Determination of the Activation Energy for the Release of Mercury from the RDF Samples

To determine the activation energy for the process of mercury being released from the RDF samples, the relationship between residence time and the amount of mercury released was determined. Example curves for sample RDF-1 are shown in Figure 3. The course of the curves for the other samples was similar. The course of the mercury release curves was typical of first-order homogeneous decomposition [46]. Based on the results, the mercury removal rate constants were determined according to Equation (2).

$$\frac{\Delta Hg}{\Delta Hg_{max}} = 1 - e^{-kt} \quad , \quad (2)$$

where

ΔHg is the mercury release after time t (-);

ΔHg_{max} is the maximum mercury release (-);

t is the reaction time (min);

k is the mercury release coefficient (min^{-1}).

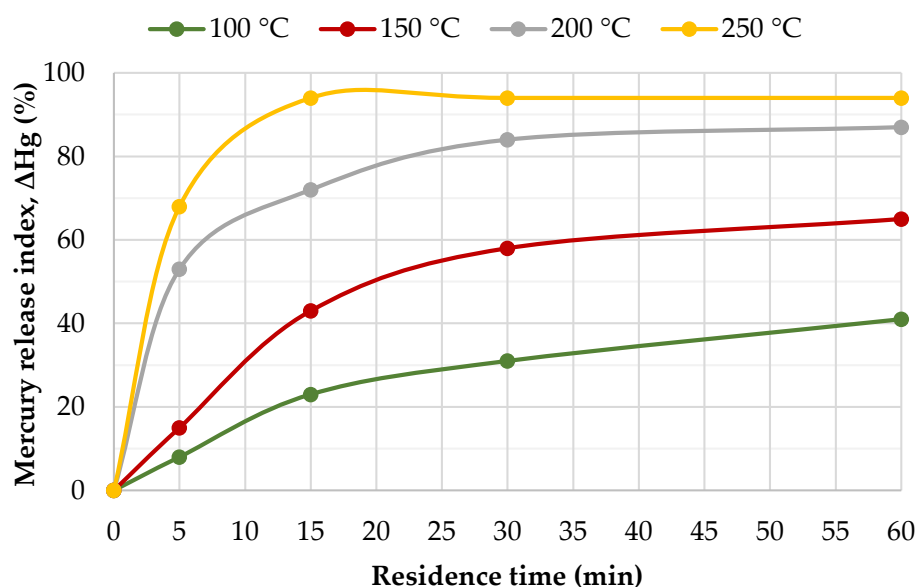


Figure 3. Effect of residence time at final temperature on the release of mercury from Sample RDF-1 (purge gas flow: $500 \text{ cm}^3/\text{min}$).

Through analogy with processes determined by temperature and time, such as the drying process [47], the Arrhenius equation was used to characterize the mercury release process. The activation energy was determined using a linear form of this equation (Equation (3)) [46,48].

$$\ln k = \ln A - \frac{E_a}{R} \cdot \frac{1}{T} \quad , \quad (3)$$

where

E_a is the activation energy (kJ/mol);

A is the pre-exponential factor (min^{-1});

R is the universal gas constant (kJ/(mol·K));

T is the temperature (K).

The activation energy of the mercury being released from the RDF samples ranged from 25.6 to 46.2 kJ/mol. The results were in accordance with our previous work [33]. A compensatory effect was observed for these results (Figure 4). The increase in activation energy (E_a) was compensated for by a simultaneous increase in the pre-exponential factor (A). A statistically significant linear relationship was observed ($R^2 = 0.985$). This linear

trend may suggest that regardless of the initial mercury content, sample characteristics, or morphological composition, the course of mercury release for all the RDF samples was similar.

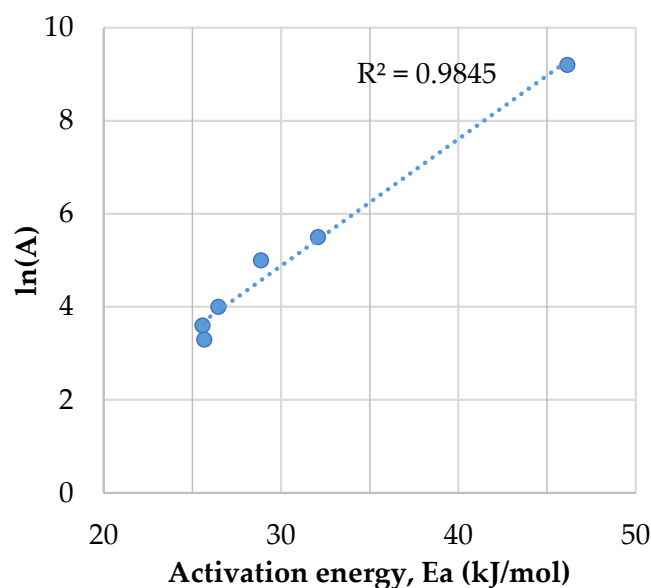


Figure 4. Relationship between the pre-exponential factor and activation energy for the RDF samples.

3.4. Statistical Analysis of the Influence of the RDF Samples' Composition on the Amount of Mercury Released

Spearman's rank order correlation coefficients for the relationship between the characteristics of the RDF samples and the amount of mercury released, as well as the activation energy of the mercury release process, are presented in the Supplemental Data (Table S1). Analysis was carried out for the maximum amount of mercury released at both 250 °C and the selected temperature ranges. The influence of the morphological composition, fuel parameters (ash content, volatile matter, sulfur content, and initial mercury content), and mass loss during the thermal treatment process were examined. A significant correlation coefficient was obtained for only two cases: (i) the amount of mercury released at 250 °C correlated with the mercury content in the RDF sample, and (ii) the amount of mercury released in the temperature range of 100–200 °C correlated with the paper (positive correlation) and plastic content (negative correlation).

Linear correlation coefficients were determined for cases with significant Spearman's rank correlation coefficients (Supplemental Data, Table S2). A significant correlation coefficient ($R = 0.888$) was obtained only for the relationship between the content of waste paper in the RDF samples and the amount of mercury released at a temperature of 100–200 °C (Figure 5). In accordance with our previous work [33], mercury was released relatively easily from various types of paper. The relationships for two other cases are shown in the Supplemental Data (Figures S1 and S2).

The relatively low correlation coefficients obtained in the statistical analysis can be explained by RDF's significant heterogeneity and the variability in the proportions of individual morphological fractions (a graphical comparison is shown in Supplemental Data, Figure S3). The heterogeneity of the RDF samples is magnified by variability in the mercury content within the three most important waste fractions: paper [36], plastics [49], and textiles [50].

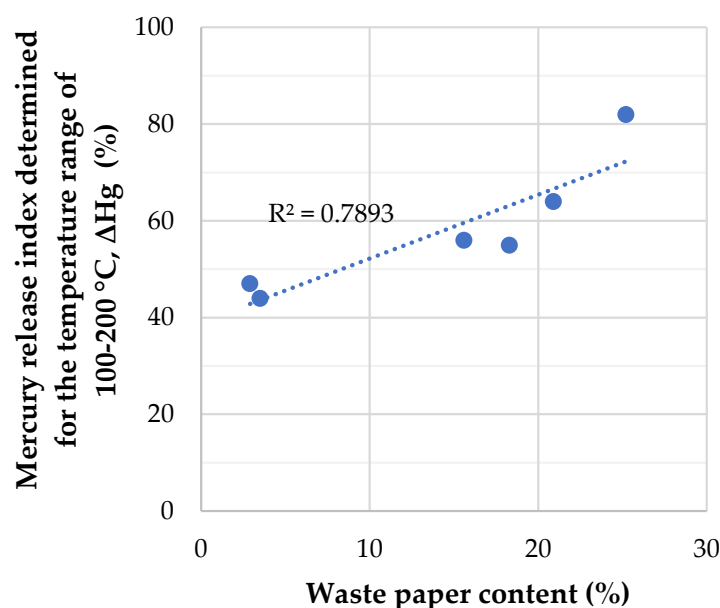


Figure 5. Relationship between the mercury release index, determined at a temperature of 100–200 °C, and the waste paper content of the RDF samples.

3.5. Limitations for Mercury Removal from RDF in Thermal Pretreatment Process

A limitation of mercury removal from RDF in the thermal pretreatment process is the necessity to remove mercury from process gases. This can be performed using sorbents. Spent sorbents are hazardous waste that requires disposal, which is mainly carried out in landfill [51]. This will result in additional operational costs. However, the proposed method is less costly than mercury removal from flue gases [52]. The cost of mercury removal from flue gases using activated carbon injection technology (LCA) is USD 110,000–150,000 per kilogram of mercury removed (assuming the effectiveness of mercury removal of 90% [53]). The mercury concentration in the processed gases derived from the thermal pretreatment process is 25 to 35 times higher than in the flue gases [54]. This will simplify the removal of mercury. Additionally, a fixed bed can be used instead of sorbent injection [55], which will reduce sorbent consumption. There is also the possibility of using regenerated sorbents [56].

The energy consumption in the thermal pretreatment of the RDF is an important issue. This will result in the generation of additional CO₂ emissions into the atmosphere. However, it should be noted that the low-mercury RDF produced will be used as a substitute for coal. The CO₂ emission factor for municipal waste incineration is approximately 60% lower than for coal combustion processes [57]. This is due to the high content of the biodegradable fraction in municipal waste, and the energy generated is classified as a renewable energy source [58]. Total CO₂ emissions from the process of power generation process from RDF fuel taking into account the emissions resulting from the thermal preparation process should still be lower than those resulting from the coal combustion process. The determination of emission factors requires a detailed life cycle assessment analysis.

Another limitation of the process is a significant reduction in the moisture content in RDF. For the examined samples, the moisture content after the thermal pretreatment process ranged from 0.7 to 2.5%. On the one hand, this is beneficial because it increases the calorific value of the fuel [7]. On the other hand, the low moisture content may pose a necessity for the use of a binder to make high-strength briquettes. For example, agro-waste [59] or glycerin [60] can be used for this purpose. This issue requires further investigation.

4. Conclusions

The RDF samples showed a very high variation in mercury content, ranging from 45 to 849 µg Hg/kg (1.7 to 35.3 µg Hg/MJ). The thermal pretreatment released a significant amount of the mercury at 250 °C (94–99%), reducing the mercury content to less than

37 µg/kg (less than 1.6 µg Hg/MJ), with a relatively low mass loss, from 3% to 13%. After the process, the SRF classification for the mercury content of the RDF samples changed to Class 1.

Appropriate waste management can be very useful in reducing mercury emissions from coal combustion processes. This can be achieved by substituting low-quality lignite and sub-bituminous coals with low-mercury RDF. In the case of RDF with high mercury content, it is possible to reduce the mercury content before combustion in the thermal pretreatment process.

Despite the differences in the characteristics of the samples in the study, in all cases, mercury began to be released at 100 °C and was almost completely released at 250 °C. The statistical analysis showed that the amount of mercury released from the samples was determined by the initial mercury content and the content of the waste paper and plastic fractions. A higher proportion of the paper fraction led to a higher amount of mercury being released in the temperature range of 100–200 °C. A higher proportion of the plastic fraction unfavorably affected the process. The relatively low correlation coefficients obtained in the statistical analysis can be explained by the significant heterogeneity of the RDF samples and variability in the mercury content within particular fractions.

Supplementary Materials: The following supporting information can be downloaded at: <https://www.mdpi.com/article/10.3390/en16020772/s1>, Figure S1: Relationship between the mercury release index at a temperature of 100–200 °C and the proportion of plastic film and plastics in the RDF samples; Figure S2: Relationship between the mercury release index determined at 250 °C and the mercury content in the RDF samples; Figure S3: Variability in the content of morphological fractions in the RDF samples; Table S1: Spearman's rank correlation coefficients for the relationship between the composition of the RDF samples and the amount of mercury released and the activation energy of the mercury released (critical value of the test: 0.886). Statistically significant coefficients are shown in bold on a gray background ($\alpha = 0.05$); Table S2: Correlation coefficients of the linear function $y = f(x)$ for the relationship between the composition of the RDF samples and the amount of mercury released (analysis performed for cases of statistically significant Spearman's rank order coefficients—Table S1). Statistically significant coefficients are shown in bold on a gray background ($\alpha = 0.05$).

Author Contributions: Conceptualization, M.B. and T.D.; methodology, T.D.; formal analysis, M.B.; investigation, M.B.; resources, M.B.; data curation M.B. and T.D.; writing—original draft preparation, M.B.; writing—review and editing, M.B., T.D., K.B. and P.B.; visualization, M.B. and T.D.; supervision, P.B.; project administration, P.B.; funding acquisition, P.B. All authors have read and agreed to the published version of the manuscript.

Funding: This research project was supported by the program “Excellence initiative—research university” for the AGH University of Science and Technology.

Data Availability Statement: The data that support the findings of this study are available from the corresponding author upon reasonable request.

Conflicts of Interest: The authors declare no conflict of interest.

References

1. Kaza, S.; Yao, L.C.; Bhada-Tata, P.; van Woerden, F. What a Waste 2.0. In *What a Waste 2.0: A Global Snapshot of Solid Waste Management to 2050*; World Bank Publications: Washington, DC, USA, 2018. [CrossRef]
2. World Energy Outlook 2021—Analysis—IEA. Available online: <https://www.iea.org/reports/world-energy-outlook-2021> (accessed on 14 December 2022).
3. Psomopoulos, C.S.; Kiskira, K.; Kalkanis, K.; Leligou, H.C.; Themelis, N.J. The Role of Energy Recovery from Wastes in the Decarbonization Efforts of the EU Power Sector. *IET Renew. Power Gener.* **2022**, *16*, 48–64. [CrossRef]
4. Chavando, J.A.M.; Silva, V.B.; Tarelho, L.A.C.; Cardoso, J.S.; Eusébio, D. Snapshot Review of Refuse-Derived Fuels. *Util. Policy* **2022**, *74*, 101316. [CrossRef]
5. Jewiarz, M.; Mudryk, K.; Wróbel, M.; Fraczek, J.; Dziedzic, K. Parameters Affecting RDF-Based Pellet Quality. *Energies* **2020**, *13*, 910. [CrossRef]
6. Gerassimidou, S.; Velis, C.A.; Williams, P.T.; Komilis, D. Characterisation and Composition Identification of Waste-Derived Fuels Obtained from Municipal Solid Waste Using Thermogravimetry: A Review. *Waste Manag. Res.* **2020**, *38*, 942–965. [CrossRef] [PubMed]

7. Dziok, T.; Bury, M.; Bytnar, K.; Burmistrz, P. Possibility of Using Alternative Fuels in Polish Power Plants in the Context of Mercury Emissions. *Waste Manag.* **2021**, *126*, 578–584. [[CrossRef](#)] [[PubMed](#)]
8. Rezaei, H.; Yazdanpanah, F.; Lim, C.J.; Sokhansanj, S. Pelletization Properties of Refuse-Derived Fuel—Effects of Particle Size and Moisture Content. *Fuel Process. Technol.* **2020**, *205*, 106437. [[CrossRef](#)]
9. Pawłowski, P.; Bałazińska, M.; Ignasiak, K.; Robak, J. Preparation of the Selected Groups of Waste Their Energy Use—Fuel from Waste Type SRF—Pieczę Przemysłowe & Kotły—Tom Nr 4 (2016)—BazTech—Yadda. Available online: <http://yadda.icm.edu.pl/baztech/element/bwmeta1.element.baztech-e47428b1-ef35-4fce-81b4-5d4f7cce3866> (accessed on 14 December 2022).
10. Chatziaras, N.; Psomopoulos, C.S.; Themelis, N.J. Use of Waste Derived Fuels in Cement Industry: A Review. *Manag. Environ. Qual. Int. J.* **2016**, *27*, 178–193. [[CrossRef](#)]
11. Kogut, K.; Górecki, J.; Burmistrz, P. Opportunities for Reducing Mercury Emissions in the Cement Industry. *J. Clean. Prod.* **2021**, *293*, 126053. [[CrossRef](#)]
12. Mlonka-Mędrala, A.; Dziok, T.; Magdziarz, A.; Nowak, W. Composition and Properties of Fly Ash Collected from a Multifuel Fluidized Bed Boiler Co-Firing Refuse Derived Fuel (RDF) and Hard Coal. *Energy* **2021**, *234*, 121229. [[CrossRef](#)]
13. Chaliki, P.; Psomopoulos, C.S.; Themelis, N.J. WTE Plants Installed in European Cities: A Review of Success Stories. *Manag. Environ. Qual.* **2015**, *27*, 606–620. [[CrossRef](#)]
14. Psomopoulos, C. Residue Derived Fuels as an Alternative Fuel for the Hellenic Power Generation Sector and Their Potential for Emissions Reduction. *AIMS Energy* **2014**, *2*, 321–341. [[CrossRef](#)]
15. Hasan, M.M.; Rasul, M.G.; Khan, M.M.K.; Ashwath, N.; Jahirul, M.I. Energy Recovery from Municipal Solid Waste Using Pyrolysis Technology: A Review on Current Status and Developments. *Renew. Sustain. Energy Rev.* **2021**, *145*, 111073. [[CrossRef](#)]
16. Śpiwak, K.; Czerski, G.; Bijak, K. The Effect of Temperature-Pressure Conditions on the RDF Gasification in the Atmosphere of Steam and Carbon Dioxide. *Energies* **2021**, *14*, 7502. [[CrossRef](#)]
17. Hilber, T.; Maier, J.; Scheffknecht, G.; Agraniotis, M.; Grammelis, P.; Kakaras, E.; Glorius, T.; Becker, U.; Derichs, W.; Schiffer, H.P.; et al. Advantages and Possibilities of Solid Recovered Fuel Cocombustion in the European Energy Sector. *J. Air Waste Manag. Assoc.* **2012**, *57*, 1178–1189. [[CrossRef](#)] [[PubMed](#)]
18. Eisler, R. Mercury Hazards to Living Organisms. In *Mercury Hazards to Living Organisms*; CRC Press: Boca Raton, FL, USA, 2006; pp. 1–312. [[CrossRef](#)]
19. BAT-LCP, Commission Implementing Decision (EU) 2017/1442 of 31 July 2017 Establishing Best Available Techniques (BAT) Conclusions, under Directive 2010/75/EU of the European Parliament and of the Council, for Large Combustion Plants. Available online: <https://eur-lex.europa.eu/legal-content/EN/TXT/?uri=CELEX:32017D1442> (accessed on 14 December 2022).
20. Ummatin, K.K.; Arifianti, Q.A.M.O.; Hani, A.; Annissa, Y. Quality Analysis of Refused-Derived Fuel as Alternative Fuels in the Cement Industry and Its Evaluation on Production. In Proceedings of the 2019 International Conference on Engineering, Science, and Industrial Applications, ICESI 2019, Tokyo, Japan, 22–24 August 2019. [[CrossRef](#)]
21. Hryb, W.; Matyasik, P. Mercury Content in Refuse-Derived Fuels. *Arch. Environ. Prot.* **2018**, *44*, 65–72. [[CrossRef](#)]
22. Bhatt, M.; Chakinala, A.G.; Joshi, J.B.; Sharma, A.; Pant, K.K.; Shah, K.; Sharma, A. Valorization of Solid Waste Using Advanced Thermo-Chemical Process: A Review. *J. Environ. Chem. Eng.* **2021**, *9*, 105434. [[CrossRef](#)]
23. Zhang, Z.; Ju, R.; Zhou, H.; Chen, H. Migration Characteristics of Heavy Metals during Sludge Pyrolysis. *Waste Manag.* **2021**, *120*, 25–32. [[CrossRef](#)]
24. Gao, N.; Wang, F.; Quan, C.; Santamaria, L.; Lopez, G.; Williams, P.T. Tire Pyrolysis Char: Processes, Properties, Upgrading and Applications. *Prog. Energy Combust. Sci.* **2022**, *93*, 101022. [[CrossRef](#)]
25. Stepień, P.; Banik, C.; Kozioł, J.A.; Białowiec, A. Emission of Volatile Organic Compounds from a Carbonized Refuse-Derived Fuel. *Przemysł Chem.* **2019**, *98*, 103–105. [[CrossRef](#)]
26. Edo, M.; Skoglund, N.; Gao, Q.; Persson, P.E.; Jansson, S. Fate of Metals and Emissions of Organic Pollutants from Torrefaction of Waste Wood, MSW, and RDF. *Waste Manag.* **2017**, *68*, 646–652. [[CrossRef](#)]
27. *PN-ENISO 21640:2021*; Solid Recovered Fuels—Specifications and Classes. ISO: Geneva, Switzerland, 2021.
28. Dziok, T.; Kołodziejska, E.K.; Kołodziejska, E.L. Mercury Content in Woody Biomass and Its Removal in the Torrefaction Process. *Biomass Bioenergy* **2020**, *143*, 105832. [[CrossRef](#)]
29. Tian, Z.; Yang, Y.; Wang, L. An Improved Method for Assessing Environmental Impacts Caused by Chemical Pollutants: A Case Study in Textiles Production. *Toxicol. Ind. Health* **2020**, *36*, 228–236. [[CrossRef](#)] [[PubMed](#)]
30. Velusamy, S.; Roy, A.; Sundaram, S.; Kumar Mallick, T. A Review on Heavy Metal Ions and Containing Dyes Removal Through Graphene Oxide-Based Adsorption Strategies for Textile Wastewater Treatment. *Chem. Rec.* **2021**, *21*, 1570–1610. [[CrossRef](#)]
31. Xue, M.G.; Wang, S.F.; Huang, C.X. Determination of Heavy Metals (Pb, Cd, Cr and Hg) in Printed Paper as Food Packaging Materials and Analysis of Their Sources. *CIESC J.* **2010**, *12*, 32.
32. Turner, A.; Filella, M. Hazardous Metal Additives in Plastics and Their Environmental Impacts. *Environ. Int.* **2021**, *156*, 106622. [[CrossRef](#)]
33. Dziok, T.; Bury, M.; Burmistrz, P. Mercury Release from Municipal Solid Waste in the Thermal Treatment Process. *Fuel* **2022**, *329*, 125528. [[CrossRef](#)]
34. Cheng, L.; Wang, L.; Geng, Y.; Wang, N.; Mao, Y.; Cai, Y. Occurrence, Speciation and Fate of Mercury in the Sewage Sludge of China. *Ecotoxicol. Environ. Saf.* **2019**, *186*, 109787. [[CrossRef](#)]

35. Iwashita, A.; Tanamachi, S.; Nakajima, T.; Takanashi, H.; Ohki, A. Removal of Mercury from Coal by Mild Pyrolysis and Leaching Behavior of Mercury. *Fuel* **2004**, *83*, 631–638. [[CrossRef](#)]
36. Bury, M.; Dziok, T. Mercury Content in Paper Waste and Possibility of Its Reduction. *Przemysł Chem.* **2021**, *100*, 77–79. [[CrossRef](#)]
37. Pilar, L.; Borovec, K.; Szeliga, Z.; Górecki, J. Mercury Emission from Three Lignite-Fired Power Plants in the Czech Republic. *Fuel Process. Technol.* **2021**, *212*, 106628. [[CrossRef](#)]
38. Rujido-Santos, I.; Herbello-Hermelo, P.; Barciela-Alonso, M.C.; Bermejo-Barrera, P.; Moreda-Piñeiro, A. Metal Content in Textile and (Nano)Textile Products. *Int. J. Environ. Res. Public Health* **2022**, *19*, 944. [[CrossRef](#)]
39. Santos-Echeandía, J.; Rivera-Hernández, J.R.; Rodrigues, J.P.; Moltó, V. Interaction of Mercury with Beached Plastics with Special Attention to Zonation, Degradation Status and Polymer Type. *Mar. Chem.* **2020**, *222*, 103788. [[CrossRef](#)]
40. Xin, F.; Xiao, R.; Zhao, Y.; Zhang, J. Surface Sulfidation Modification of Magnetospheres from Fly Ash for Elemental Mercury Removal from Coal Combustion Flue Gas. *Chem. Eng. J.* **2022**, *436*, 135212. [[CrossRef](#)]
41. Kawamoto, K. Adsorption Characteristics of the Carbonaceous Adsorbents for Organic Compounds in a Model Exhaust Gas from Thermal Treatment Processing. *J. Air Waste Manag. Assoc.* **2022**, *72*, 463–473. [[CrossRef](#)] [[PubMed](#)]
42. Sun, Y.; Tao, J.; Chen, G.; Yan, B.; Cheng, Z. Distribution of Hg during Sewage Sludge and Municipal Solid Waste Co-Pyrolysis: Influence of Multiple Factors. *Waste Manag.* **2020**, *107*, 276–284. [[CrossRef](#)] [[PubMed](#)]
43. Lee, W.R.; Eom, Y.; Lee, T.G. Mercury Recovery from Mercury-Containing Wastes Using a Vacuum Thermal Desorption System. *Waste Manag.* **2017**, *60*, 546–551. [[CrossRef](#)]
44. Rezić, I. *Historical Textiles and Their Characterization*; Cambridge Scholars Publishing: Newcastle upon Tyne, UK, 2022.
45. Stepień, P.; Pulka, J.; Serowik, M.; Białowiec, A. Thermogravimetric and Calorimetric Characteristics of Alternative Fuel in Terms of Its Use in Low-Temperature Pyrolysis. *Waste Biomass Valorization* **2019**, *10*, 1669–1677. [[CrossRef](#)]
46. Merdes, A.C.; Keener, T.C.; Khang, S.J.; Jenkins, R.G. Investigation into the Fate of Mercury in Bituminous Coal during Mild Pyrolysis. *Fuel* **1998**, *77*, 1783–1792. [[CrossRef](#)]
47. Koukouch, A.; Idlimam, A.; Asbik, M.; Sarh, B.; Izrar, B.; Bostyn, S.; Bah, A.; Ansari, O.; Zegaoui, O.; Amine, A. Experimental Determination of the Effective Moisture Diffusivity and Activation Energy during Convective Solar Drying of Olive Pomace Waste. *Renew. Energy* **2017**, *101*, 565–574. [[CrossRef](#)]
48. Sotiropoulou, R.E.P.; Serafidou, M.; Skodras, G. Thermal Mercury Removal from Coals: Effect of Pyrolysis Conditions and Kinetic Analysis. *Fuel* **2019**, *238*, 44–50. [[CrossRef](#)]
49. Czop, M.; Błaszczuk, E. Determination of the Fuel Properties of Selected Packaging Waste from the Municipal Sector. *Arch. Gospod. Odpad. Ochr. Środowiska* **2015**, *17*, 131–138.
50. Morshed, M.N.; Behary, N.; Bouazizi, N.; Guan, J.; Nierstrasz, V.A. An Overview on Biocatalysts Immobilization on Textiles: Preparation, Progress and Application in Wastewater Treatment. *Chemosphere* **2021**, *279*, 130481. [[CrossRef](#)] [[PubMed](#)]
51. Xu, Y.; Luo, G.; Zhang, Q.; Cui, W.; Li, Z.; Zhang, S. Potential Hazards of Novel Waste-Derived Sorbents for Efficient Removal of Mercury from Coal Combustion Flue Gas. *J. Hazard. Mater.* **2021**, *412*, 125226. [[CrossRef](#)] [[PubMed](#)]
52. Misztal, E.; Chmielniak, T.; Mazur, I.; Sajdak, M. The Release and Reduction of Mercury from Solid Fuels through Thermal Treatment Prior to Combustion. *Energies* **2022**, *15*, 7987. [[CrossRef](#)]
53. Shen, A.; Wang, Y.; Wang, R.; Duan, Y.; Tao, J.; Gu, X.; Wang, P.; Xu, Z. Numerical Simulation of Sorbent Injection into Flue Gas for Mercury Removal in Coal-Fired Power Plant. Part 2. Operational Parameters and Optimization. *Fuel* **2022**, *326*, 124990. [[CrossRef](#)]
54. Chmielniak, T. Reduction of Mercury Emissions to the Atmosphere from Coal Combustion Processes of Using Low-Temperature Pyrolysis—A Concept of Process Implementation on a Commercial Scale. *Rynek Energii* **2011**, *93*, 176–181.
55. Jastrząb, K.; Mazurek, I. The Study of Thermal Desorption of Mercury Compounds from Spent Active Cokes Used for Exhaust Gas Treatment in Waste Incineration Plants. *Inżynieria Ochr. Śr.* **2013**, *16*, 273–285.
56. Antuña-Nieto, C.; Rodríguez, E.; Lopez-Anton, M.A.; García, R.; Martínez-Tarazona, M.R. Noble Metal-Based Sorbents: A Way to Avoid New Waste after Mercury Removal. *J. Hazard. Mater.* **2020**, *400*, 123168. [[CrossRef](#)]
57. Monni, S. From Landfilling to Waste Incineration: Implications on GHG Emissions of Different Actors. *Int. J. Greenh. Gas Control* **2012**, *8*, 82–89. [[CrossRef](#)]
58. Wasielewski, R.; Bałazińska, M. Energy Recovery from Waste in the Aspect of qualifications of Electricity and Heat as Coming from Renewable Energy and to Participate in the Emissions Trading System. *Polityka Energetyczna—Energy Policy J.* **2018**, *21*, 129–142.
59. Batool, I.; Munir, S.; Khalid, A.; Tahir, A.; Munir, S. Effectiveness of Different Binders on RDF Potential from Agro Waste. *Tech. J. UET Taxila* **2021**, *26*, 38–44.
60. Jamradloedluk, J.; Lertsatitthanakorn, C. Properties of Densified-Refuse Derived Fuel Using Glycerin as a Binder. *Procedia Eng.* **2015**, *100*, 505–510. [[CrossRef](#)]

Disclaimer/Publisher’s Note: The statements, opinions and data contained in all publications are solely those of the individual author(s) and contributor(s) and not of MDPI and/or the editor(s). MDPI and/or the editor(s) disclaim responsibility for any injury to people or property resulting from any ideas, methods, instructions or products referred to in the content.